

## Functional multicomponent metal oxide films based on Sr, Sn, Fe and Mo in the anodic alumina matrices

*Gennady Gorokh\*, Anna Zakhlebayeva, Andrei Lazavenka, Nikolai Sobolev, Valery Zhylinski, Nataliya Bogomazova, Marta Yarmolich, Nikolai Kalanda*

((Optional Dedication))

Dr. G.G. Gorokh, A.I. Zakhlebayeva, A.A. Lazavenka  
Belarusian State University of Informatics and Radioelectronics, P. Brovki str. 6, Minsk  
220013, Belarus  
E-mail: [gorokh@bsuir.by](mailto:gorokh@bsuir.by)

Dr. N.A. Sobolev  
Aveiro University, Campus Universitário de Santiago, Aveiro 3810-193, Portugal

Dr. V.V. Zhylinski, Dr. N.V. Bogomazova  
Belarusian State Technological University, Sverdlova str. 13a, Minsk 220006, Belarus

Dr. M.V. Yarmolich, Dr. N.A. Kalanda  
Scientific-Practical Materials Research Centre, NAS of Belarus, P. Brovki str. 19, Minsk  
220072, Belarus

Keywords: nanostructures, chemical deposition, sol-gel method, anodic alumina, metal oxide films

Low-profile anodic alumina matrices 1  $\mu\text{m}$  thick with pore sizes of 105 and 160 nm were formed by two-step anodizing of Al layers on Si substrates and then the formed alumina matrices were used as templates for deposition of multicomponent metal oxide films on their surfaces. The metal oxide systems of  $\text{Sr}_2\text{FeMoO}_{6-\delta}$ ,  $\text{Fe}_x\text{Mo}_y\text{O}_z$  and  $\text{Sn}_x\text{Mo}_y\text{O}_z$  composites with carbon nanotubes had been synthesized by the ion layer deposition, sol-gel and drop method with using the aqueous solutions of salts, and then the deposited films were annealed in isothermal regime at 373 – 473 K for 1-2 hours, and polythermal regime at 773 - 1123 K for 2-10 hours. The formed multicomponent metal oxides films were evenly distributed along the walls of pores and on the surfaces of the alumina matrices. The morphology, microstructure and composition of the porous alumina matrices together with multicomponent metal oxides films were examined by the scanning electron microscope, the energy dispersive X-ray microanalysis and the X-ray phase analysis. It had been shown that the use of anodic alumina matrices made it possible to reduce the dimension of grains and give uniformity to the microstructure and properties of the metal oxide films. The carbon nanotubes increased the

This article has been accepted for publication and undergone full peer review but has not been through the copyediting, typesetting, pagination and proofreading process, which may lead to differences between this version and the [Version of Record](#). Please cite this article as doi: [10.1002/pssb.201900283](https://doi.org/10.1002/pssb.201900283)

This article is protected by copyright. All rights reserved

working surface of the functional layer and its electrical conductivity. The variation in the synthesis conditions of deposited films and configuration of the anodic alumina matrices allowed to change the phase composition of synthesized metal oxide structures. The developed technique based on the use of ordered nanoporous anodic alumina matrices allows the functional films to form of different complex composition compounds with reproducible structure and properties.

## 1. Introduction

Intensive development of nanotechnological approaches is penetrating all spheres of science and production and it gives an impetus to the development of new techniques in the formation of nanostructured films and elements of the nanoscale range, ensuring the availability, manufacturability and composition reproducibility of the formed objects. <sup>[1]</sup> In modern materials science, the synthesis of composite materials with desired characteristics is a priority for the development of new technologies. Such a synthesis is carried out by combining nanostructured materials and various physicochemical processes for their production. <sup>[2]</sup> One of the most promising and popular areas of the synthesis of composite materials is the formation of multicomponent compounds, which, depending on their composition, can exhibit different properties. <sup>[3,4]</sup> The traditionally used metal oxides ( $\text{SnO}_2$ ,  $\text{ZnO}$ ,  $\text{WO}_3$ ,  $\text{In}_2\text{O}_3$ ,  $\text{MoO}_3$ ) as functional layers in chemical sensors, photovoltaics, photocatalysis, spintronics and photonics are replaced by functional nanostructured films of the combined composition ( $\text{ZnO-SnO}_2$ ,  $\text{SnO}_2\text{-WO}_3$ ,  $\text{SnO}_2\text{-MoO}_3$ ,  $\text{MoO}_3\text{-Fe}_2\text{O}_3$  etc.). Such materials are distinguished by their higher physicochemical characteristics, as well as by stability of properties and composition. <sup>[5,6]</sup> In particular, two-component metal oxides of  $\text{ZnO-SnO}_2$  and  $\text{SnO}_2\text{-WO}_3$  that were used in gas sensors have a higher sensitivity and selectivity at low concentrations of certain gases (such as  $\text{NO}_2$ ,  $\text{NO}$  and exc.) in comparison to simple oxides. The introduction of carbon tubes into the composition of metal oxide composites also makes it possible to improve their functional properties. The branched complex microstructure of composite oxide films together with carbon nanotubes ( $\text{CNT}_s$ ) increases

their adsorbing properties and the number of defect vacancies on the surfaces of composite films. <sup>[7,8]</sup>

The most attractive method of improving the metal oxides properties is the film deposition on profiled surfaces, as a result, the surface of the metal oxide films becomes nanostructured materials. Nanoporous anodic alumina matrices (NAAM) with a regular cellular-porous structure are best suited for this purpose. The use of NAAM as templates makes it possible to reduce the grain size of deposited films, to form nanostructures with controlled sizes, <sup>[9-12]</sup> as well as significantly increases the effective surface of the nanostructured film. <sup>[13,14]</sup>

Among the technological methods of film deposition, liquid-phase methods occupy an increasingly significant position as less expensive in comparison with gas-phase high-temperature or vacuum processes. <sup>[15]</sup> The most suitable and effective chemical methods for the formation of metal oxide films with a controlled composition and properties on nanoporous matrices are the method of the electrophoretic layer-by-layer deposition, <sup>[16]</sup> the ion layer deposition, <sup>[17,18]</sup> the sol-gel method <sup>[19,20]</sup> and drop method with using the aqueous solution of salts. <sup>[21]</sup> The electrophysical, chemosensitive and magnetic characteristics of such composite films are related to their structural ordering, which is determined by the presence of the regularity of the arrangement regularity of elementary crystallites. <sup>[22-24]</sup> The use of NAAM makes it possible to form a specified array of nanoclusters with controlled sizes and surface distributions. <sup>[25]</sup>

This article presents the results of the metal oxide films synthesis of Sn, Sr, Fe, and Mo by various liquid-phase methods in nanoporous anodic alumina matrices, and studies of their microstructure, composition and functional properties.

## 2. Experimental Section

### 2.1. Formation of nanoporous anodic alumina matrices (NAAM)

The nanoporous anodic alumina matrices (NAAM) were formed by two stage anodizing of the sputter-deposited onto silicon substrates aluminium films (99.99%, 1.2  $\mu\text{m}$  thick) at the current density of  $6 \text{ mA}\cdot\text{cm}^{-2}$  in malonic and tartaric acids. The anodic potentials at the first anodizing step were of 85 V for malonic and of 195 V for tartaric electrolytes. To improve pore regularity and enlarge the surface of the upper porous layer, the formed anodic alumina was removed in a selective solvent by following the procedure described in Ref. <sup>[14]</sup> This is due to the specific swelling and widening of the distances between the concaves during the compact oxide formation, which confines effectively the surface available for pore nucleation and, ultimately, makes the pores grow straight and vertical just from the film surface. The second anodizing step was done at anodic potential of 90 V and 200 V in malonic and tartaric acids respectively. The anodic alumina layer 1  $\mu\text{m}$  thick was formed on the pre-textured by anodic oxidation surface of aluminium. To increase the surface-to-volume ratio, the films were subjected to pore modification in mixture of phosphoric and chromic acids at  $T = 323 \text{ K}$  for 5 minutes. The pore diameters were about 105 nm for malonic acid and about 160 nm for tartaric acid. **Figure 1** schematically shows the sequence of technological operations for the preparation of NAAM with deposited layers of the studied metal oxides.

### 2.2. Formation compounds $\text{Sr}_2\text{FeMoO}_{6-\delta}$ by sol-gel method in NAAM

The compound of  $\text{Sr}_2\text{FeMoO}_{6-\delta}$  system was prepared by the sol-gel method, using  $\text{Sr}(\text{NO}_3)_2$ ,  $\text{Fe}(\text{NO}_3)_3 \times 9\text{H}_2\text{O}$ ,  $(\text{NH}_4)_6\text{Mo}_7\text{O}_{24}$  and  $\text{C}_6\text{H}_8\text{O}_7 \times \text{H}_2\text{O}$  as starting materials. <sup>[19]</sup> At first, the aqueous solutions of  $\text{Sr}(\text{NO}_3)_2$  ( $0.4 \text{ mol}\cdot\text{dm}^{-3}$ ) and  $\text{Fe}(\text{NO}_3)_3$  ( $2 \text{ mol}\cdot\text{dm}^{-3}$ ) were mixed in a molar ratio 2(Sr):(Fe), and then  $\text{C}_6\text{H}_8\text{O}_7 \cdot \text{H}_2\text{O}$  was added to the solution in a molar ratio 6.5( $\text{C}_6\text{H}_8\text{O}_7 \cdot \text{H}_2\text{O}$ ):(Fe). After this,  $(\text{NH}_4)_6\text{Mo}_7\text{O}_{24}$  solution ( $0.2 \text{ mol}\cdot\text{dm}^{-3}$ ) was added to the

prepared solution in a molar ratio (Mo):(Fe). By adding of ethylenediamine (EDA) into two parts of this solution their pH values were adjusted to 4 and 9, correspondently. In previous works, we had shown that the synthesis of  $\text{Sr}_2\text{FeMoO}_{6-\delta}$  powders obtained at the solution with a pH of 4 allowed to obtain films with maximum superstructural ordering, but the raising of pH decreased the degree of order superstructure.<sup>[19]</sup> Finally, the obtain solutions were continuously stirred at 353K until the light green gels had been formed. The formed gels were deposited to the NAAM by centrifugation and then their structures were crystallised by three-step annealing. The first stage of gel heating up to 473K was carried out by the polythermal regime at rate of 0.4 deg/min. Then the samples were hold at this temperature for 2 hours.<sup>[19]</sup> The second stage, the formed composite systems were annealed in air at partial pressure of oxygen of  $p\text{O}_2 = 0.21 \times 10^5$  Pa at  $T = 773$  K for 8 hours to form the  $\text{Sr}_2\text{FeMoO}_{6-\delta}$  film distributed over the porous oxide surface. In order to obtain  $\text{Sr}_2\text{FeMoO}_{6-\delta}$  with structural ordering of  $\text{Fe}^{3+}$  and  $\text{Mo}^{5+}$  cations  $\text{Sr}_2\text{FeMoO}_{6-\delta}$  compound were annealed in a continuous stream of 5%  $\text{H}_2/\text{Ar}$  (gas mixture: 5% $\text{H}_2$  + 95% $\text{Ar}$ ) by means of a polythermic approach from 773 to 1273 K with a 2 deg/min heating rate and holding at this temperature for 10 hours.

### 2.3. Formation carbon-containing composites of $\text{Sn}_x\text{Mo}_y\text{O}_z$ and $\text{Fe}_x\text{Mo}_y\text{O}_z$ in NAAM

Carbon-containing composites were formed by sequential deposition of carbon nanotubes (CNT) and metal oxides in NAAM. First, the carbon nanotubes suspension (1%) in propylenecarbonate (Cnano Technology Limited Company) was sprayed on the NAAM defatted surface at the rate of 1 ml per 1  $\text{cm}^2$ . Then, the prepared composites were dried in air at  $T = 313$  K for 1 hours. The metal oxide systems of  $\text{Sn}_x\text{Mo}_y\text{O}_z$  were formed by electrophoretic deposition of molybdenum and tin hydroxides.<sup>[16,21]</sup> The  $\text{Sn}(\text{OH})_2$  films were prepared by electrophoretic deposition on NAAM from an aqueous solution of  $\text{K}_2[\text{Sn}(\text{OH})_4]$  ( $0.01 \text{ mol} \cdot \text{dm}^{-3}$ ; pH = 8) at field potential of  $V = 50$  V, current frequency of  $f = 50$  Hz and

inter electrode spacing of  $h = 200$  mm. To make the oxidations of  $\text{Sn}^{2+}$  to  $\text{Sn}^{4+}$ , the resulting films were annealed in air at  $T = 623$  K for 2 hours. Further, the molybdate ions were deposited on the resulting film from an aqueous solution of  $(\text{NH}_4)_2\text{MoO}_4$  ( $0.01 \text{ mol}\cdot\text{dm}^{-3}$ ;  $\text{pH} = 5$ ) at field potential of  $V = 50$  V, frequency of  $f = 50$  Hz and inter electrode spacing of  $h = 200$  mm. Then, the prepared films of the insoluble tin polymolybdates were annealed at  $T = 1023$  K during 0.5 hours for forming the  $\text{Sn}_x\text{Mo}_y\text{O}_z$  compounds.

The semiconductor layers of the molybdenum and iron oxides were precipitated by dropping from aqueous solutions of  $(\text{NH}_4)_6\text{Mo}_7\text{O}_{24} \cdot 4\text{H}_2\text{O}$  (1%) and  $\text{FeSO}_4 \cdot 7\text{H}_2\text{O}$  (1%) on top of CNT layer ( $0.3 \text{ ml}\cdot\text{cm}^{-2}$ ). The prepared samples were then annealed in argon at  $T = 1023$  K for 0.5 hour.

#### 2.4. Analysis methods of functional multicomponent metal oxide films

The surface morphology and cross-sections as well as energy dispersive X-ray microanalysis that colored mapping of the NAAM with metal oxides films were examined in a Hitachi S-806 scanning electron microscope (SEM) operated at 15 kV of accelerated voltage.

The crystal lattice parameters and a degree of the superstructural ordering of cations were determined by using ICSD–PDF2 (Release 2000) database and POWDERCELL<sup>[26]</sup>

FullProf<sup>[27]</sup> software by the Rietveld technique on the basis of the XRD data was obtained by the Philips X'Pert MPD diffractometer in conditions of the Cu-K $\alpha$  radiation at room temperature. XRD patterns were measured at room temperature at the rate of 60 deg/h in the 10–90 deg angular range.

### 3. Results and discussion

#### 3.1. Investigation of strontium ferromolybdate films in NAAM

Schematic and SEM images of the cross-sections of NAAM with  $\text{Sr}_2\text{FeMoO}_{6-\delta}$  films after different annealing steps are shown in **Figure 2**. The used citrate-gel method made it possible to fill the pores of the nanoporous matrices with a gel-like solution. Under annealing at the moderate temperature at  $T = 373 - 473$  K for 2 hours, the solvent was evaporated and the compound was compacted and evenly filled the deep of the pores (**Figure 2, a**). As a result of annealing at  $T = 773$  K for 8 hours, compound was evenly distributed along the walls of the pores (**Figure 2, b**). After high-temperature annealing at  $T = 1123$  K for 10 hours, the multicomponent metal oxide was transformed into grains on the inner surface of the pore walls (**Figure 2, c**).

The results of the energy dispersive X-ray microanalysis of  $\text{Sr}_2\text{FeMoO}_{6-\delta}$  films synthesized in NAAM are shown in **Figure 3**. In spectrum, we detected elements that belong to the substrate with the NAAM – Al (1.432 eV), O (0.56 eV), Si (1.77 eV) – and synthesized in the pores of the metal oxide composite  $\text{Sr}_2\text{FeMoO}_{6-\delta}$  – Fe (0.637 eV, 6.4 eV, 7.05 eV), Sr (1.82 eV), Mo (2.32 eV). The element composition of synthesized composites was 23.34 mas% of Fe, 58.96 mas % of Sr and 17.70 mas % of Mo, and atomic ratio was 32.77 at% of Fe, 52.76 at % of Sr and 14.47 at % of Mo.

According to XRD data,  $\text{Sr}_2\text{FeMoO}_{6-\delta}$  compounds annealed at  $T = 773$  K are multiphase oxides with the contents of the  $\text{SrMoO}_4$ ,  $\text{SrCO}_3$  and  $\text{Fe}_3\text{O}_4$  phases. The phase percentage of nanocomposites formed from solutions with  $\text{pH} = 4$  and  $\text{pH} = 9$ , depending on the annealing temperature, is shown in **Figure 4**.

The phase transformations investigations of the  $\text{Sr}_2\text{FeMoO}_{6-\delta}$  compound in the process of crystallization in the polythermic mode at  $T = 773 - 1123$  K showed that the synthesis of a solid solution from the stoichiometric mixture  $\text{Sr}(\text{NO}_3)_2$ ,  $\text{Fe}(\text{NO}_3)_3 \cdot 9\text{H}_2\text{O}$ ,  $(\text{NH}_4)_6\text{Mo}_7\text{O}_{24}$  proceeds through the series of parallel stages. At the initial stage, the resulting  $\text{Sr}_2\text{FeMoO}_{6-\delta}$

films are enriched with iron. With an increase of temperature during the course of chemical processes, the composite composition changes in the direction of increasing the content of molybdenum, which leads to a change in the parameters of the crystal lattice. During a preliminary synthesis, in the polythermal mode, when the temperature raised at 2 K/min to  $T = 893$  K, the decomposition of the  $\text{SrMoO}_4$  intermediate phase began and reached 100% of  $\text{Sr}_2\text{FeMoO}_{6-x}$  phase transformation up to  $T = 1063$  K. With the increase of the annealing temperature to  $T = 1123$  K the final synthesis of  $\text{Sr}_2\text{FeMoO}_{6-x}$  is completed. The reflections of the  $\text{Sr}_2\text{FeMoO}_{6-\delta}$  compound predominate on the X-ray diffraction patterns.

The temperature dependences of the specific magnetization of the formed composites were measured in pre-cooling modes up to  $T = 4.2$  K in a magnetic field  $B = 0.01$  T (FC – field cooling) and without it (ZFC – zero-field cooling), followed by heating in a magnetic field (**Figure 5**). The comparative analysis of the temperature-magnetic dependences of composites obtained from the solutions with  $\text{pH} = 4$  and  $\text{pH} = 9$  showed that the magnetic state of the formed systems is influenced by the microstructure of  $\text{Sr}_2\text{FeMoO}_{6-\delta}$  and the degree of superstructural ordering of  $\text{Fe}^{3+}$ ,  $\text{Mo}^{5+}$  cations. The presence of antisite defects [FeMo] and [MoFe] in the composition of composites obtained from a solution with  $\text{pH} = 9$  affects the magnitude of the magnetization of the structures at  $T = 4.2$  K  $M \sim 1,27 \mu_B/\text{f.u}$  ( $\text{pH} = 9$ ), while  $M_{\text{sat}} \sim 2,47 \mu_B/\text{f.u}$  ( $\text{pH} = 4$ ). This could be explained by the  $\text{Sr}_2\text{FeMoO}_{6-\delta}$  composites, obtained from the solution with  $\text{pH} = 4$ , that are characterized by more uniform magnetic structure. A sharp increase in the structures of magnetization in the temperature range  $T = 4.2\text{--}35$  K indicates the presence of magnetic regions with a low coercive force, which are nanoscale grains and their exchange forces ensure uniform magnetization and contribute to the observed superparamagnetic state.

Thus, varying the composition of the gel-forming solutions and the heat treatment regimes of the formed systems allows the directional change in the phase composition of the synthesized nanoscale magnetic structures. The formation of ferrimagnetic nanocluster arrays with

required and controlled sizes with the help of NAAM in predetermined manner opens the broad prospects for creating magnetically ordered systems with predictable properties.

### 3.2. Investigation of nanocomposites based on carbon nanotubes with $\text{Fe}_x\text{Mo}_y\text{O}_z$ in NAAM

The surfaces and cross-sections of the NAAM with the thin film system of CNT/ $\text{Fe}_x\text{Mo}_y\text{O}_z$  before and after annealing were presented in the **Figure 6**. The scattering electron microscope studies have shown that after drying the resulting coating we get a homogeneous system, in which the CNT penetrates the metal oxide film and exits to the surface (**Figure 6 a, c**). After annealing (**Figure 6 b, d**) the film is compacted on the surface and in the pores of anodic alumina matrix, the CNTs are exposed above the film and increase the working surface of the functional layer and its electrical conductivity. Thus, the surface resistance of metal oxide films on the CNTs decreased from  $1.6 \text{ M}\Omega\cdot\text{cm}$  to  $300 \text{ k}\Omega\cdot\text{cm}$ . The change in the electrophysical parameters of composite films occurs due to the formation of bonds between the CNTs and molybdenum oxide compounds, such as:  $\text{CNT} - (\text{COO})^{-2}\text{MoO}_4^{-2}$  and  $\text{CNT} - (\text{COO})^{-2}\text{MoO}_3^{-2}$ .

The results of the energy dispersive X-ray microanalysis showed the presence of molybdenum, oxygen and iron, which indicates the metal-oxide character of the formed semiconductor oxide film (**Figure 7**).

In addition, after annealing the porous structure of anodic alumina matrix filled with CNT and semiconductor metal oxide layer is clearly manifested, in which predominant molybdenum oxides (19.24%) are doped with iron (1.44%). The elemental analysis showed a ratio of Fe : Mo as 0.45 at% : 3.33 at%  $\approx 2 : 7$ , which indicates probably the formation of  $\text{Fe}_2\text{Mo}_7\text{O}_{24}\times(\text{H}_2\text{O})_x$  film on the surface of CNT (47 at%) and NAAM (Al – 2.64 at% , O<sub>2</sub> – 46.2 at%). It should be noted that the metal oxide film completely fills the pores of NAAM between the CNTs. In NAAM

### 3.3. Investigation of nanocomposites based on carbon nanotubes with $\text{Sn}_x\text{Mo}_y\text{O}_z$ in NAAM

**Figure 8** shows representative SEM images of the surfaces and cross-sections of NAAM with deposited systems of  $\text{CNT}/\text{Sn}_x\text{Mo}_y\text{O}_z$  before (**Figure 8 a, c**) and after (**Figure 8 b, d**) annealing.

After annealing, the porous structure of the NAAM filled with the CNTs and semiconductor oxide is clearly manifested. The CNTs do not penetrate the pores, and thus, show low adhesion between oxide layer and the NAAM. The array of the CNTs on which the crystalline phases of molybdenum and tin oxides were formed, as in the case of applying  $\text{Fe}_x\text{Mo}_y\text{O}_z$ , increases the effective surface of the thin film and its electrical conductivity. This is due to the increased catalytic activity of CNTs, where oxidation occurs faster than on pure oxide. In both cases, salts of tin and iron are used as precursors in the precipitation of molybdenum, and they form sparingly soluble salts with  $\text{MoO}_4^{2-}$  and  $\text{MoO}_3^{2-}$ .

Elemental analysis showed the ratio Sn : Mo as 0.19 at% : 3.54 at%  $\approx$  3 : 7, that indicates the formation of  $\text{Sn}_3\text{Mo}_7\text{O}_{24} \times (\text{H}_2\text{O})_x$  film on the CNT surface (37 at%) and alumina (Al – 3.47 at% and O<sub>2</sub> – 55.6 at%).

The results of X-ray phase analysis of  $\text{CNT}/\text{Sn}_x\text{Mo}_y\text{O}_z$  synthesized in NAAM (**Figure 9**) indicate the presence of crystalline phases of  $\text{MoO}_3$  and  $\text{MoO}_2$  in the formed structures. At the same time, crystalloids of individual iron and tin oxides were not found, which probably indicates the dissolution of iron and tin ions in the molybdenum oxide matrix. It should be noted that the  $\text{CNT}/\text{Sn}_x\text{Mo}_y\text{O}_z$  system is characterized by the large broadening of the peaks for the  $\text{MoO}_2$  phase, which reflects the great defectiveness of this structure. The decomposition of  $\text{Sn}_3\text{Mo}_7\text{O}_{24} \times \text{H}_2\text{O}$  and  $\text{Fe}_2\text{Mo}_7\text{O}_{24} \times \text{H}_2\text{O}$  salts during the synthesis was carried out together with the process of disproportionation of  $\text{Mo}^{6+}$  to  $\text{Mo}^{4+}$ , which is reflected by the presence of  $\text{MoO}_2$  peaks on the X-ray diagram.

These results confirm the fact that the  $\text{Al}_2\text{O}_3/\text{CNT}/\text{Fe}_x\text{Mo}_y\text{O}_z$  and  $\text{Al}_2\text{O}_3/\text{CNT}/\text{Sn}_x\text{Mo}_y\text{O}_z$  systems on the arrays of carbon nanotubes with crystalline oxides  $\text{MoO}_3$  and  $\text{MoO}_2$  are precipitated on their surface, and they are doped with iron and tin ions.

#### 4. Conclusion

Nanoporous matrices of anodic aluminum oxide with a thickness of 1  $\mu\text{m}$  with pore sizes of 105 and 160 nm were used as templates to deposit the multicomponent metal oxides based on Sr, Sn, Fe and Mo compounds using various liquid-phase methods, such as the ion layering, the sol-gel method and the dropping from the solutions. The formed matrix composites were subjected to multi-stage polythermal and isothermal treatments in oxygen and oxygen-free environments at different temperatures to produce nanostructured functional metal oxide systems.

The prepared compound of  $\text{Sr}_2\text{FeMoO}_{6-\delta}$  system by the sol-gel method, using  $\text{Sr}(\text{NO}_3)_2$ ,  $\text{Fe}(\text{NO}_3)_3 \cdot 9\text{H}_2\text{O}$ ,  $(\text{NH}_4)_6\text{Mo}_7\text{O}_{24}$  and  $\text{C}_6\text{H}_8\text{O}_7 \cdot \text{H}_2\text{O}$ , and then annealed process at temperatures of 353-473K, 473-773 K had a fine-grained structure and stoichiometric composition of strontium ferromolybdate. The atomic ratio of the elements in the composition of the synthesized composites was 32.77 at% of Fe, 52.76 at % of Sr and 14.47 at % of Mo. According to XRD data, the annealed  $\text{Sr}_2\text{FeMoO}_{6-\delta}$  compounds in the temperature range of 773-1273 K after completion of phase transformations represent magnetically ordered systems with superparamagnetic state.

The nanostructured composites based on  $\text{Fe}_x\text{Mo}_y\text{O}_z$  and carbon nanotubes in NAAM are characterized by the high effective surface and increased electrical conductivity compared with similar metal oxide films. This occurs due to bonding between the CNTs and molybdenum oxide compounds. The energy dispersive X-ray microanalysis showed the presence of molybdenum, oxygen and iron, which indicates the metal-oxide character of the

formed semiconductor oxide film. The presence of additional bonds and the developed surface show the promise of such composites as active layers of chemical sensors.

The X-ray phase analysis of the synthesized carbon-containing composites  $\text{Sn}_x\text{Mo}_y\text{O}_z$  in NAAM indicates the presence of crystalline phases of  $\text{MoO}_3$  and  $\text{MoO}_2$ . The array of CNT with the crystalline phases of molybdenum and tin oxides, as in the case of  $\text{Fe}_x\text{Mo}_y\text{O}_z$ , increases the effective surface of the prepared thin film and its electrical conductivity. This is due to the increased catalytic activity of CNTs, where oxidation occurs faster than on pure oxide. In both cases, salts of tin and iron are used as precursors in the precipitation of molybdenum, and they form sparingly soluble salts with  $\text{MoO}_4^{2-}$  and  $\text{MoO}_3^{2-}$ . The structures of the systems of  $\text{Al}_2\text{O}_3/\text{CNT}/\text{Fe}_x\text{Mo}_y\text{O}_z$  and  $\text{Al}_2\text{O}_3/\text{CNT}/\text{Sn}_x\text{Mo}_y\text{O}_z$  are followed by the carbon nanotubes with crystalline oxide phases of  $\text{MoO}_3$  and  $\text{MoO}_2$ , which have been precipitated on their surface, and have been doped with iron and tin ions.

The developed chemical methods for the formation of nanostructured functional multicomponent metal oxide films based on Sr, Sn, Fe and Mo in the nanoporous anodic alumina allow to change the phase composition and properties of synthesized metal oxide structures by variation of the qualitative and quantitative composition of the aqueous solutions of salts, the heat treatment regimes and the nanoporous matrices configurations.

The formed multicomponent films can be used as the chemosensitive layers of promising gas sensors and sensory microsystems, the magnetoresistive films of magnetically operated devices for electronic engineering, as well as the photosensitive layers of optoelectronic devices.

### **Acknowledgements**

The work was supported by the State program of scientific research of the Republic of Belarus “Physical materials science, new materials and technologies, project 1.2.3” and grant №4.1.07 of the State program of scientific research “Electroplating” approved by the

resolution No. 55 of the Presidium of the National Academy of Sciences of Belarus of  
30.11.2015.

Received: ((will be filled in by the editorial staff))

Revised: ((will be filled in by the editorial staff))

Published online: ((will be filled in by the editorial staff))

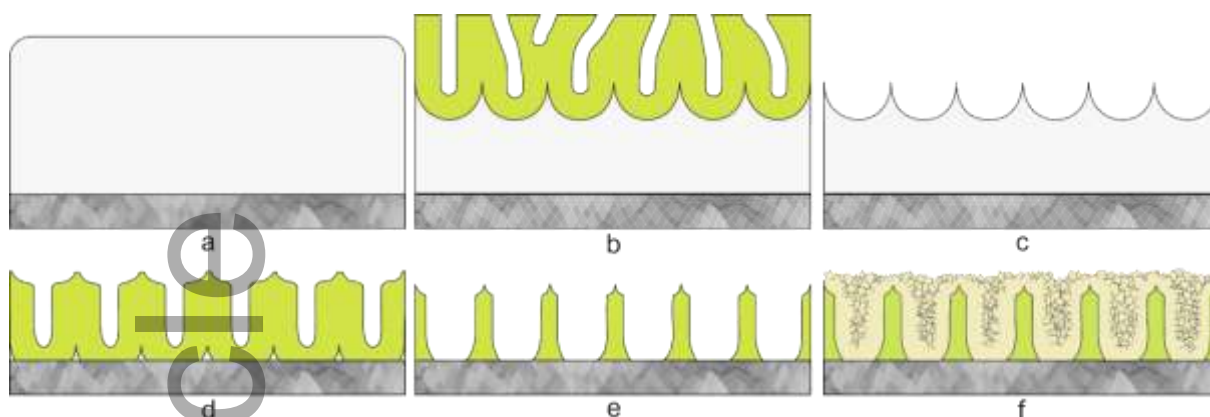
## References

- [1] L. F. Fraceto, R. de Lima, H. C. Oliveira, D. S. Ávila, B. Chen, *Energ. Ecol. Environ.* **2018**, 3, 69.
- [2] K. Miyazaki, N. Islam, *Technovation*. **2007**, 27, 661.
- [3] T. Kumpika, E. Kantarak, W. Sroila, A. Panthawan, P. Sanmuangmoon, W. Thongsuwan, P. Singjaia, *Optik*. **2017**, 133, 114.
- [4] A. Arfaouia, A. Mhamdi, N. Besrour, S. Touihri, H.I. Ouzari, Z. A. Alrowailia, M. Amlouk, *Thin Solid Films*. **2018**, 648, 12.
- [5] B. Mondal, B. Basumatari, J. Das, C. Roychaudhury, H. Saha, & N. Mukherjee, *Sensors and Actuators B: Chemical*. **2014**, 194, 389.
- [6] N. V. Toan, C. M. Hung, N. V. Duy, N. D. D. T. T. Hoa, Le, & N. V. Hieu, *Materials Science and Engineering: B*. **2017**, 224, 163.
- [7] R. B. Ladani, S. Wu, A. J. Kinloch, K. Ghorbani, J. Zhang, A. P. Mouritz, C. H. Wang, *Compos. Sci. Technol.* **2015**, 117, 146.
- [8] H. Gu, Y. Li, N. Li, *Fibers Polym.* **2015**, 16, 122601.
- [9] W. Lee, S.-J. Park, *Chem. Rev.* **2014**, 114, 7487–7556.
- [10] A. Y. Polyakov, A. V. Markov, M. V. Mezhenyi, A. V. Govorkov, V. F. Pavlov, N. B. Smirnov, A. A. Donskov, L. I. D'yakonov, Y. P. Kozlova, S. S. Malakhov, T. G. Yugova, V. I. Osinsky, G. G. Gorokh, N. N. Lyahova, V. B. Mityukhlyayev, S. J. Pearton, *Appl. Phys. Lett.* **2009**, 94(2), 022114.
- [11] Z. Cheng, L. Sun, Z. Y. Li, P. Serbun, N. Kargin, V. Labunov, B. Shulitski, I. Kashko, D. Grapov, G. Gorokh, *World J. Res. Rev.* **2017**, 4(3), 8.

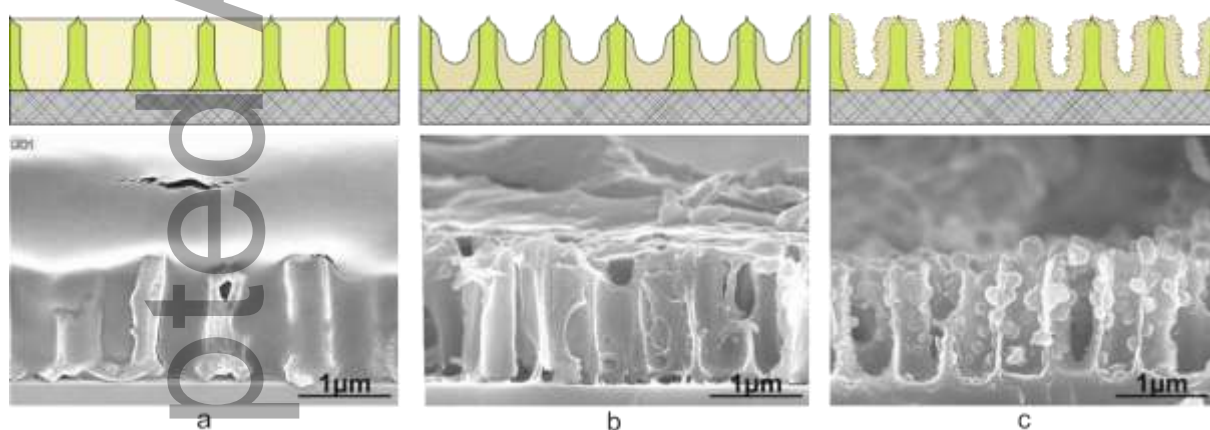
- [12] G. G. Gorokh, A. A. Lozovenko, L. P. Bulat, *Semiconductors*. **2017**, 51(7), 850.
- [13] G. G. Gorokh, M. I. Pashechko, J. T. Borc, A. A. Lozovenko, I. A. Kashko, A. I. Latos, *Appl. Surf. Sci.* **2018**, 43, 829.
- [14] V. Khatko, G. Gorokh, A. Mozalev, D. Solovei, E. Llobet, X. Vilanova. X. Correig, *Sensors and Actuators B: Chemica*. **2006**, 118, 255.
- [15] A. Pyanko, V. Zhilinskiy, G. Gorokh, in *Promising materials and processes in technical electrochemistry*, Monograph (Eds: V. Z. Barsukov, Yu. V. Borysenko, O. I. Buket, V. G. Khomenko), KNUTD, Kyiv, Ukraine **2016**, P. 185.
- [16] G. Gorokh, A. Zakhlebayaeva, V. Zhilinskiy, A. Pyanko, presented at 26<sup>th</sup> Int. Crim. Conf. «Microwave & Telecommunication Technology», Sevastopol, Ukraine, September, **2016**.
- [17] N. Bogomazova, G. Gorokh, A. Zakhlebayaeva, A. Pligovka, A. Murashkevich, T. Galkovsky, *J. Phys.: Conf. Ser.* **2018**, 1124, 021083.
- [18] V. P. Tolstoy, L. B. Gulina, *Thin Solid Films*. **2003**, 1-2, 74.
- [19] M. Yarmolich, N. Kalanda, S. Demyanov, H. Terry, J. Ustarroz, M. Silibin, G. Gorokh, *Beilstein J. Nanotechnol.* **2016**, 7, 1202.
- [20] D. B. Ashok, S. Sachin, G. A. Sawant, C. M. Mahajan, *J. Nano- Electron. Phys.* **2015**, 4, 1.
- [21] G. G. Gorokh, A. I. Zakhlebayaeva, A. I. Metla, V. V. Zhilinskiy, A. N. Murashkevich, N. V. Bogomazova, *J. Phys.: Conf. Ser.* **2017**, 917, 092011.
- [22] A. Pligovka, A. Lazavenka, A. Zakhlebayaeva, presented at IEEE NANO 2019, Int. Conf. Nanotechnology, Cork, Ireland, July, **2019**.
- [23] V. Khatko, A. Mozalev, G. Gorokh, D. Solovei, F. Guirado, E. Llobet, X. Correig, *J. Electrochem. Soc.* **2008**, 155(7), K116.
- [24] N. A. Kalanda, G. G. Gorokh, M. V. Yarmolich, A. A. Lozovenko, E. Y. Kanyukov, *Phys. Sol. State*. **2016**, 58(2), 351.

- [25] V. F. Surganov, G. G. Gorokh, *SPIE*. **2000**, 4019, 526.
- [26] W. Kraus, G. Nolze, *J. Appl. Cryst.* **1996**, 29, 301.
- [27] J. Rodriguez-Carvajal, *Newsletter of the Powder Diffraction Commission of the International Union of Crystallography*, **2001**, 26, 12.

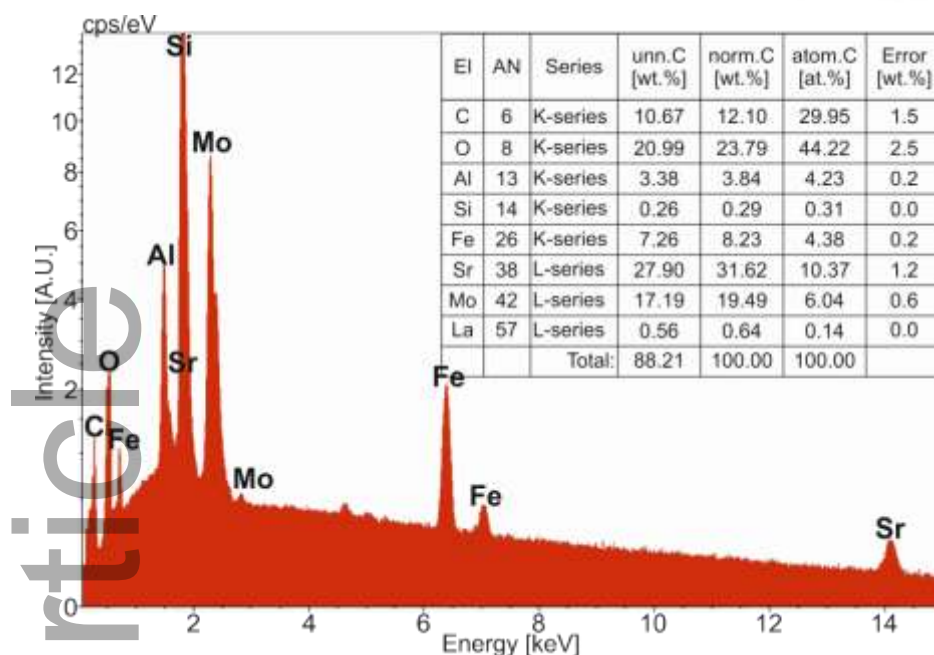
Accepted Article



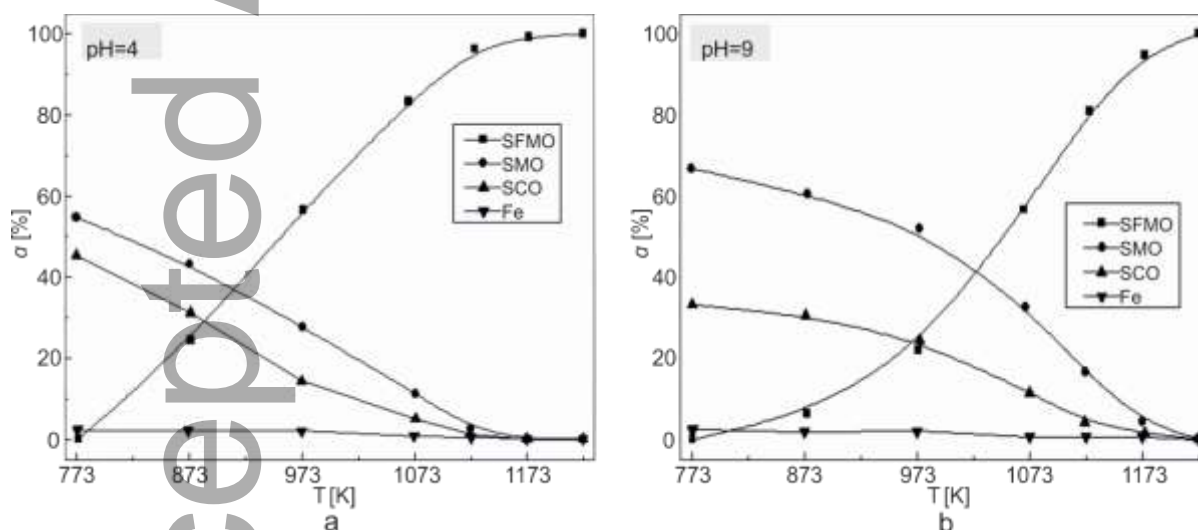
**Figure 1.** The technological operations sequence for the preparation of NAAM with deposited metal oxide layers: **(a)** deposition of Al on a Si substrate; **(b)** the first anodizing step; **(c)** selective dissolution of the anodic alumina; **(d)** the second anodizing step; **(e)** the expansion of the pores of the anodic alumina; **(f)** matrix filling with metal oxide compound



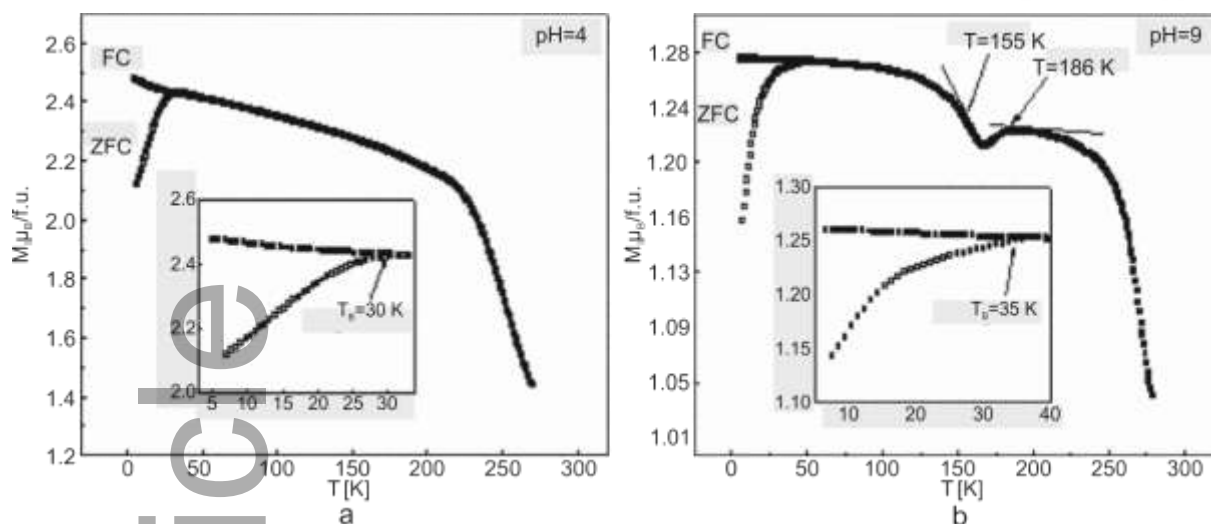
**Figure 2.** Schematic and SEM images of the cross-sections of NAAM with  $\text{Sr}_2\text{FeMoO}_{6-\delta}$  after different annealing steps: **(a)**  $T = 373\text{-}473\text{ K}$ ,  $t = 2\text{ h}$ ; **(b)**  $p\text{O}_2 = 0.21 \times 10^5\text{ Pa}$ ,  $T = 773\text{ K}$ ,  $t = 8\text{ h}$ ; **(c)**  $5\% \text{ H}_2/\text{Ar}$ ,  $T = 1123\text{ K}$ ,  $t = 10\text{ h}$



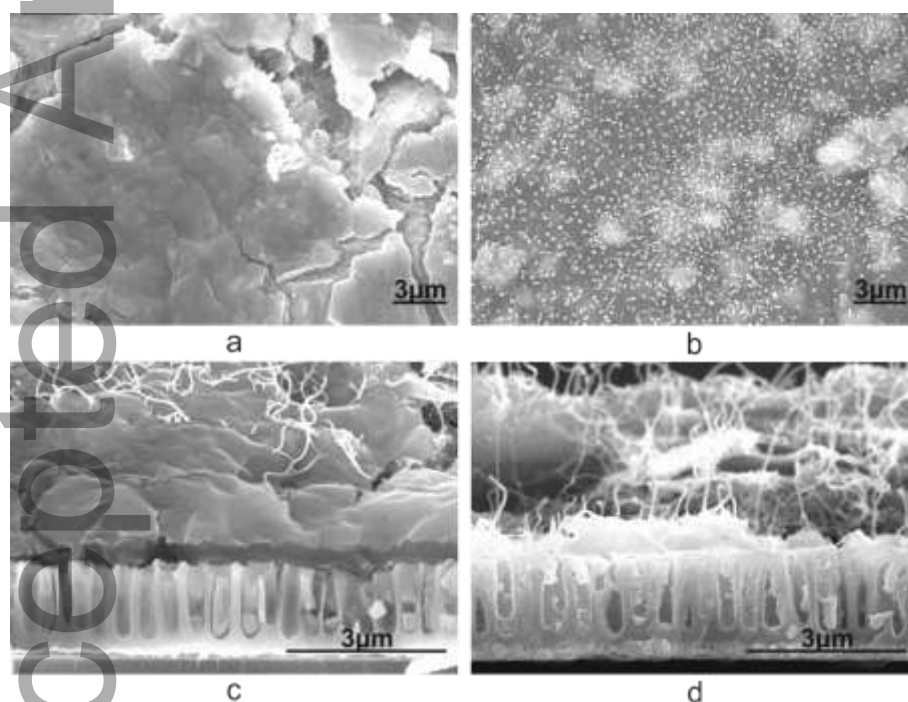
**Figure 3.** The energy dispersive X-ray spectrum of  $\text{Sr}_2\text{FeMoO}_{6-\delta}$  synthesized in NAAM by the sol-gel method



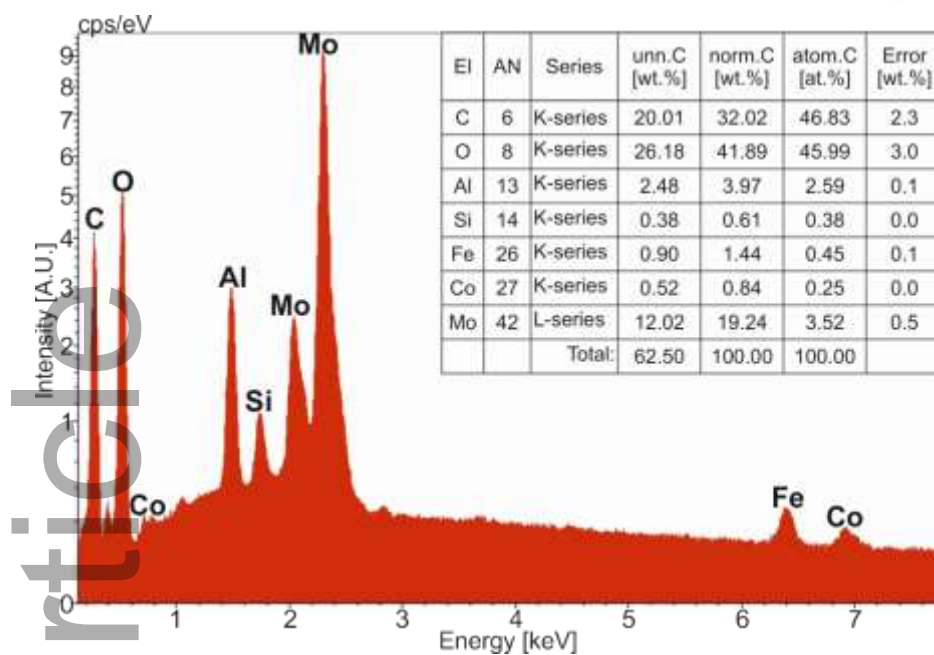
**Figure 4.** The percentage of phases  $\text{SrMoO}_4$ ,  $\text{SrCO}_3$ ,  $\text{Fe}_3\text{O}_4$  in composites formed from solutions with pH = 4 (a), pH = 9 (b)



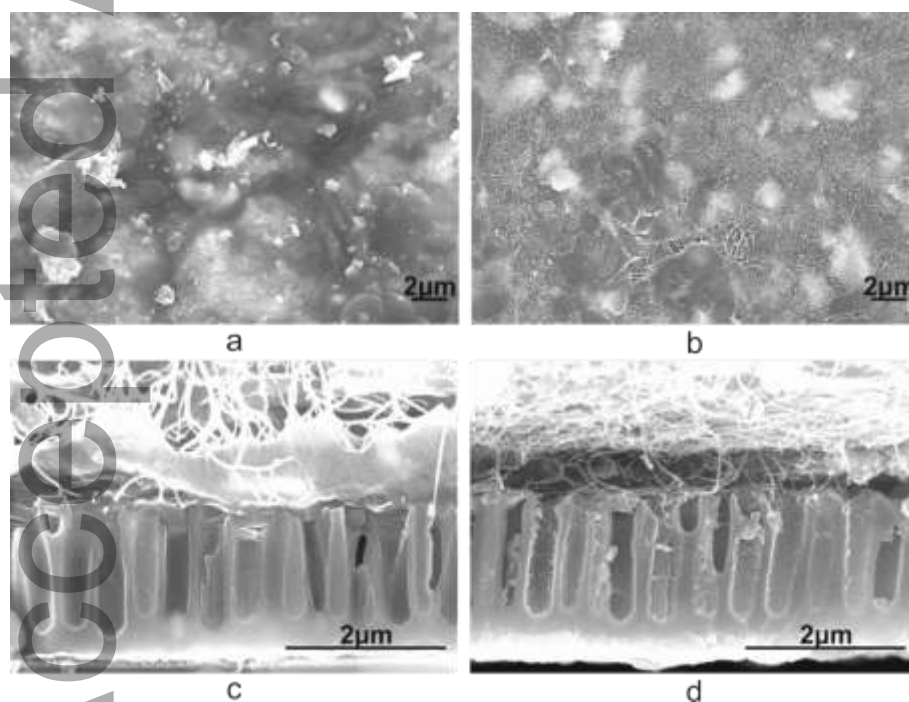
**Figure 5.** The temperature dependences of the composites magnetization formed from solutions with pH = 4 (a), pH = 9 (b)



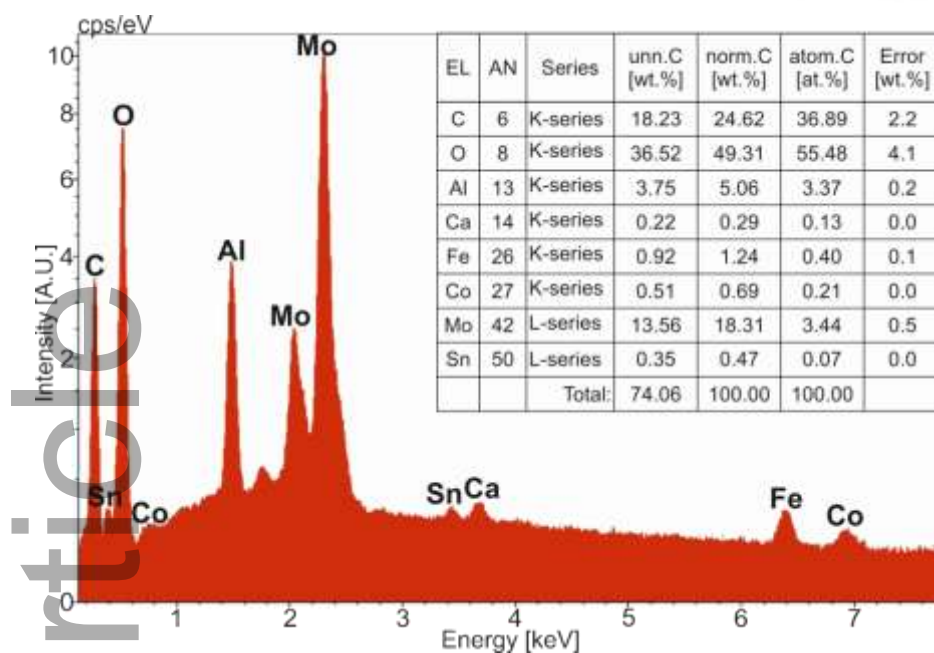
**Figure 6.** SEM images of surfaces (a,b) and the cross-sections (c,d) of NAAM with CNT/Fe<sub>x</sub>Mo<sub>y</sub>O<sub>z</sub> before (a,c) and after (b,d) annealing at  $T = 1123$  K during 0.5 h



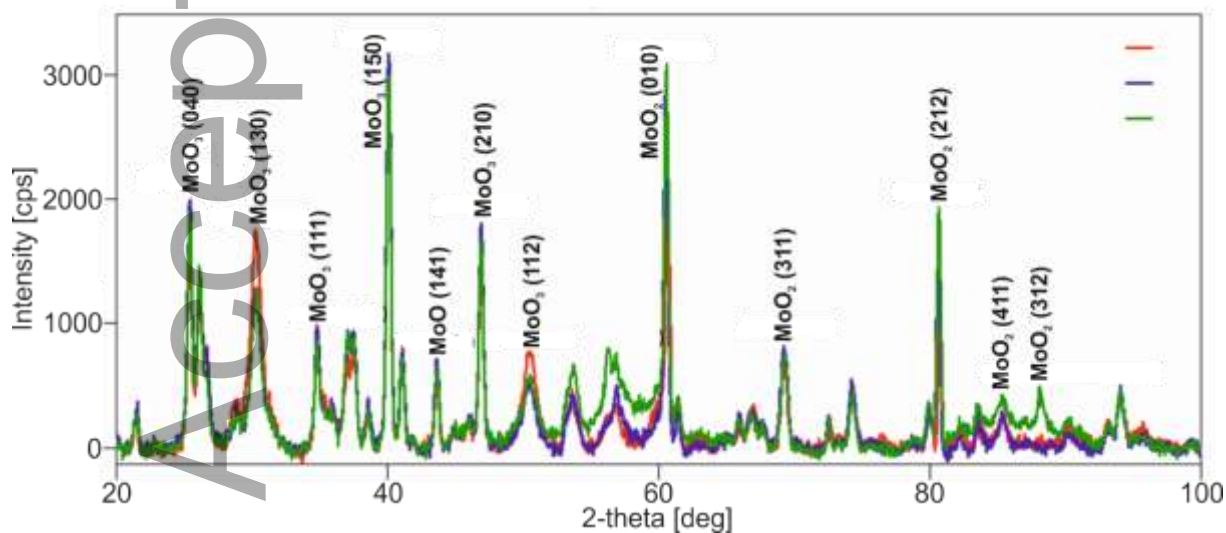
**Figure 7.** The results of the energy dispersive X-ray microanalysis of NAAM with CNT/Fe<sub>x</sub>Mo<sub>y</sub>O<sub>z</sub>



**Figure 8.** SEM images of surfaces (**a,b**) and the cross-sections (**c,d**) of NAAM with CNT/Sn<sub>x</sub>Mo<sub>y</sub>O<sub>z</sub> before (**a,c**) and after (**b,d**) annealing  $T = 1123$  K, during 0.5 h



**Figure 9.** The results of the energy dispersive X-ray microanalysis of NAAM with CNT/Sn<sub>x</sub>Mo<sub>y</sub>O<sub>z</sub>

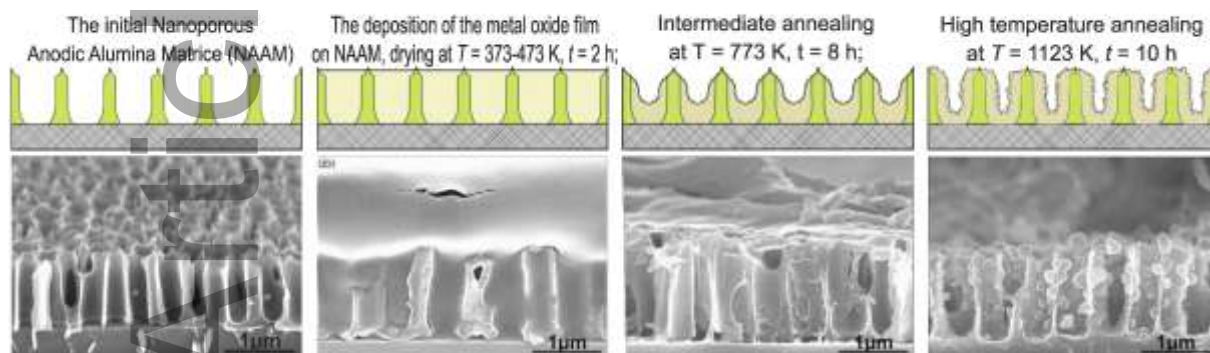


**Figure 10.** X-ray phase analysis of CNT/Sn<sub>x</sub>Mo<sub>y</sub>O<sub>z</sub> synthesized in NAAM

**Short summary**

Nanostructured metal oxide composite films of the composition Sr, Sn, Fe, and Mo were formed in porous templates of anodic alumina.

The microstructure, composition and properties of the obtained functional films were investigated. Prospects for the use of the investigated films as functional materials for devices of the new generation were shown.

**The method of obtaining functional metal oxide films**

Accepted Article